

## TWO-PHASE FLOW PATTERNS VISUALIZATION OF CARBON DIOXIDE IN A MICROCHANNEL

### José Luiz Gasche

UNESP – São Paulo State University, College of Engineering at Ilha Solteira  
Department of Mechanical Engineering  
Av. Brasil Centro 56, Ilha Solteira-SP, 15385-000, Brazil  
e-mail: [gasche@dem.feis.unesp.br](mailto:gasche@dem.feis.unesp.br)

### Anthony M. Jacobi

UIUC – University of Illinois at Urbana-Champaign  
Department of Mechanical and Industrial Engineering  
1206 West Green Street, Urbana, IL 61801, USA  
e-mail: [a-jacobi@uiuc.edu](mailto:a-jacobi@uiuc.edu)

*Abstract.* It is well known that carbon dioxide is a very interesting alternative for replacing chlorofluorocarbons (CFCs), hydrochlorofluorocarbons (HCFCs), and hydrofluorocarbons (HFCs) since it is non-flammable, non-toxic, inexpensive and widely available, and does not affect the global environment. In addition, CO<sub>2</sub> has excellent thermo physical properties, leading to good heat transfer, efficient compression, and compact systems design due to high volumetric capacity. Despite its importance for designing evaporators and condensers, a review of the open literature shows that heat transfer data during phase change of carbon dioxide is very limited, mainly for microchannel flows. This paper will contribute to the subject of flow visualization of CO<sub>2</sub> vaporization inside a 0.8 mm-hydraulic diameter microchannel. A total of 28 tests were performed at saturation temperature of 23.3°C for one heat flux of 1800 W/(m<sup>2</sup>·°C). Vapor qualities ranged from 1 to 81% and mass flux ranged from 58 to 235 kg/(m<sup>2</sup>·s). The results showed three flow patterns. For low vapor qualities (up to about 25%), plug flow was predominant, while slug flow appeared to occur at moderated vapor qualities (from about 25 to 50%). Annular flow was speculated to be the flow pattern for higher qualities.

*Keywords.* Carbon Dioxide, Boiling, Visualization, Flow Pattern

### 1. Introduction

It is widely known that the synthetic halocarbons used in refrigerating and air-conditioning systems are now phased out owing to their negative impact on the global environment. Promising alternatives for refrigeration technology are substances called by natural fluids, because of their negligible global warming potential (GWP). Among these fluids one can mention refrigerants like the hydrocarbons, ammonia, and carbon dioxide. If non-toxic and non-flammable fluid is required, carbon dioxide (CO<sub>2</sub>) is a competitive refrigerant and has gained much attention recently.

In addition, CO<sub>2</sub> has excellent thermo physical properties. Carbon dioxide has a much smaller surface tension and liquid viscosity. Bubble formation is facilitated due to the decreased surface tension, resulting in higher boiling heat transfer coefficient, while a smaller pressure drop can be found due to the decreased liquid viscosity. The properties of the critical point (31°C and about 74 bar) also indicate that the pressure level is far higher in CO<sub>2</sub> systems than in conventional systems, requiring the development of suitable components. On the other hand, the high-pressure level permits the design of systems with small component dimensions and low compression ratios, which improve compressor efficiency.

As mentioned by Cavallini (1996), carbon dioxide has been successfully used in a prototype automotive air conditioner (an application with high relative direct global warming impact when using HFC134a), and excellent prospects are also predicted in commercial refrigerating units with associated tap-water heating, and in high-temperature-range heat pumps.

Compact heat exchangers for CO<sub>2</sub> can be obtained if small diameter channels are used. Channels having a hydraulic diameter of less than 2 mm are usually named microchannels. The high heat transfer coefficient and significant potential in decreasing the heat exchanger surface area are the major advantages of using this kind of geometry. Therefore, compact and lightweight heat exchangers can be designed with microchannels. For these reasons microchannel heat exchangers have been used in bioengineering and microelectronics as well as in evaporators and condensers of refrigeration systems.

The heat transfer performance of the evaporator is one of the important features of the successful operation of a refrigeration unit. Since the optimum design of the evaporator depends on the correct evaluation of the heat transfer characteristics of the flow during the phase change of the refrigerant, the knowledge of data on two-phase flow and heat transfer is essential.

Studies on two-phase flow and heat transfer in microchannel geometries have mostly been focused on low-pressure refrigerants, and air/water systems at atmospheric pressure. Even for conventional fluids, the knowledge of microchannel flow and heat transfer is limited, Pettersen (2001). There are a few previous works on systematic experimental investigation of carbon dioxide heat transfer and its modeling.

Good reviews of microchannel heat transfer can be found in Zhao et al. (2000), Pettersen (2001), and Palm (2001). Zhao et al. (2000) presented a review of microchannel heat transfer for single-phase and two-phase (condensation and

evaporation) forced convection. In this work they presented a short review of CO<sub>2</sub> heat transfer, from which one can conclude that most authors have studied CO<sub>2</sub> heat transfer for channels of large diameters (from about 5 mm to 11 mm). In this review only Pettersen et al. (1998) had experimentally evaluated the overall heat transfer coefficient in microchannel heat exchanger. Zhao et al. (2000) also performed a series of experiments to study flow boiling of CO<sub>2</sub> in microchannels. The experiments were conducted to investigate the effect of mass flux ( $G$ ) and heat flux ( $q$ ) on the boiling heat transfer coefficient ( $h$ ) and pressure drop. The experiments were conducted for mass flux from 250 to 700 kg/(m<sup>2</sup>s), heat flux from 8 to 25 kW/m<sup>2</sup>, and saturation temperatures from 5 to 15°C. The vapor quality ( $x$ ) of all tests was 0.05. They did not present the dimensions of the microchannel. The preliminary results showed that the effects of mass flux and heat flux on heat transfer coefficient were negligible. It was also found that the thermal-hydraulic performance of CO<sub>2</sub> was superior to R134a.

Pettersen (2001) presented a good review of CO<sub>2</sub> evaporation heat transfer and pressure drop for large-diameter flow as well as for microchannel flow. He mentioned that earlier studies on CO<sub>2</sub> evaporation heat transfer for large diameter flow were performed by Bredesen et al. (1997), Hogaard Knudsen and Jensen (1997), Rieberer (1998), Sun and Groll (2001), and Yun et al. (2001). On microchannel flow, heat transfer data for CO<sub>2</sub> were obtained by Hihara and Tanaka (2000), Zhao et al. (2000), Ohadi et al. (2000), and Koyama et al. (2001). Pettersen (2001) commented that the results presented by these authors were obtained by different experimental methods and for various operational conditions and have shown certain discrepancies among the data. Pettersen (2001) also conducted heat transfer tests in a rig using a flat, extruded aluminum microchannel tube of 540 mm length with 25 channels of 0.81 mm diameter. The test tube was heated by a water jacket in order to get representative boundary conditions for air-to-refrigerant heat transfer ("fluid heating"). Vaporization heat transfer and pressure drop data were recorded over a wide range of conditions, including temperatures from 0 to 25°C, heat flux from 5 to 20 kW/m<sup>2</sup>, mass flux from 190 to 570 kg/(m<sup>2</sup>s), and vapor qualities between 0.2 and 0.8. Test results showed that the nucleate boiling mechanism dominated at low/moderate vapor qualities, where the heat transfer coefficient increased with heat flux and temperature, but was less affected by varying mass flux and vapor fraction. Heat transfer coefficients ranging from about 10 to 20 kW/(m<sup>2</sup>K) were measured in this region. Dryout effects became very important at higher mass flux and temperature, where  $h$  dropped rapidly at increasing  $x$ . A special rig was also built in order to observe two-phase flow patterns. A horizontal quartz glass tube with internal diameter of 0.98 mm coated by transparent resistive coating of indium tin oxide was used to perform the tests. Two-phase flow patterns were recorded mainly at a temperature of 20°C, and mass flux ranging from 100 to 580 kg/(m<sup>2</sup>s). The observation showed a dominance of intermittent (slug) flow at low vapor qualities, and wavy annular flow with entrainment of droplets at higher  $x$ . At high mass flux, the annular/entrained flow pattern was described as dispersed. Stratified flow was not observed in the tests with heat load. The nucleate (pool) boiling correlation of Gorenflo (1993) gave the best fit to the experimental data; values 8% above the test data on average (using a reference coefficient of 4170 W/(m<sup>2</sup>K)).

Palm (2001) also presented a good review on heat transfer in microchannels. He stated that for two-phase flow, very little information was available for microchannels. Especially, the size range below 1 mm had been investigated by only a few researchers, most of them concerning evaporation. Related to CO<sub>2</sub> evaporation in microchannels, Palm (2001) mentioned only the work performed by Zhao et al. (2000), commented on earlier in this work. He concluded from this review that flow boiling was governed mainly by nucleate boiling mechanisms in the diameter range below about 4 mm. A pool boiling correlation such as Coopers' gave reasonable but conservative values for heat transfer coefficient as long as the critical heat flux was not reached. Like Pettersen (2001), he also concluded that there were still many open questions to be answered before reliable design tools were available in the form of correlating equations for heat transfer and pressure drop and suggested that more research was needed in this field.

The present work aims to help to improve the understanding of CO<sub>2</sub> evaporation in microchannels. Among the few works in this area we found experimental results performed by Hiraha and Tanaka (2000) and Koyama et al. (2001), who utilized only one stainless steel tube in order to obtain the heat transfer coefficient. However, they did not perform the flow visualization, an important characteristic when dealing with phase change. As mentioned by Thome (2001), the best approaches for modeling two-phase heat transfer and two-phase pressure drops are based on two-phase flow pattern analysis. Zhao et al. (2000), and Ohadi et al. (2000) used a test rig containing several parallel microchannels, which introduce an additional variable to the problem; the flow distribution through the microchannels. Like Hiraha and Tanaka (2000), and Koyama et al. (2001), they also did not perform the flow visualization. Only Petersen (2001) presented results for both, heat transfer coefficient and flow visualization. But even Petersen (2001) did not perform the tests in a same test rig. The heat transfer coefficients were measured in a test rig containing several microchannels and the flow visualization tests were performed in a different test rig using a glass tube in order to permit the visual access to the flow. With these conditions, the heat transfer data and the flow visualization results cannot be exactly interrelated. In this work, a test rig with a single microchannel was developed in order to permit both the measurement of the heat transfer coefficient and the visualization of the flow in the same experimental setup. Only the flow visualization results are presented in this work.

## 2. Experimental Method

### 2.1. Overview

A once-through, open-loop, CO<sub>2</sub> delivery system was designed by Aldana (2000), and modified in this work, to allow control of the CO<sub>2</sub> thermodynamic state entering the test section inlet. The test loop is shown in Figure 1. The CO<sub>2</sub> source was a 9.1 kg liquid-CO<sub>2</sub> cylinder with a central riser tube that allowed liquid to be syphoned from the cylinder bottom. Electric heating blankets were used to increase the CO<sub>2</sub> cylinder temperature and pressure to a desired value. Once a target pressure was reached, the regulator was opened and CO<sub>2</sub> flowed down a chilled inlet section, named subcooler, ensuring subcooled liquid entered the preheater. The preheater was an electric heater with a copper tube wound around it, and was used to set a desired vapor quality at the inlet of the test section. Mass flow rate was calculated from the decrease in source-cylinder mass over time. The pressure difference in the CO<sub>2</sub> superheated vapor flow through a capillary tube installed at the end of the test loop was used for monitoring the mass flow rate. Throttle valves in the exhaust line were used to adjust the desired mass flow rate. Transducer data allowed monitoring of flow conditions, and were imputed into a PC-based Data Acquisition System (DAS). Specific aspects of the test loop are described as follows.

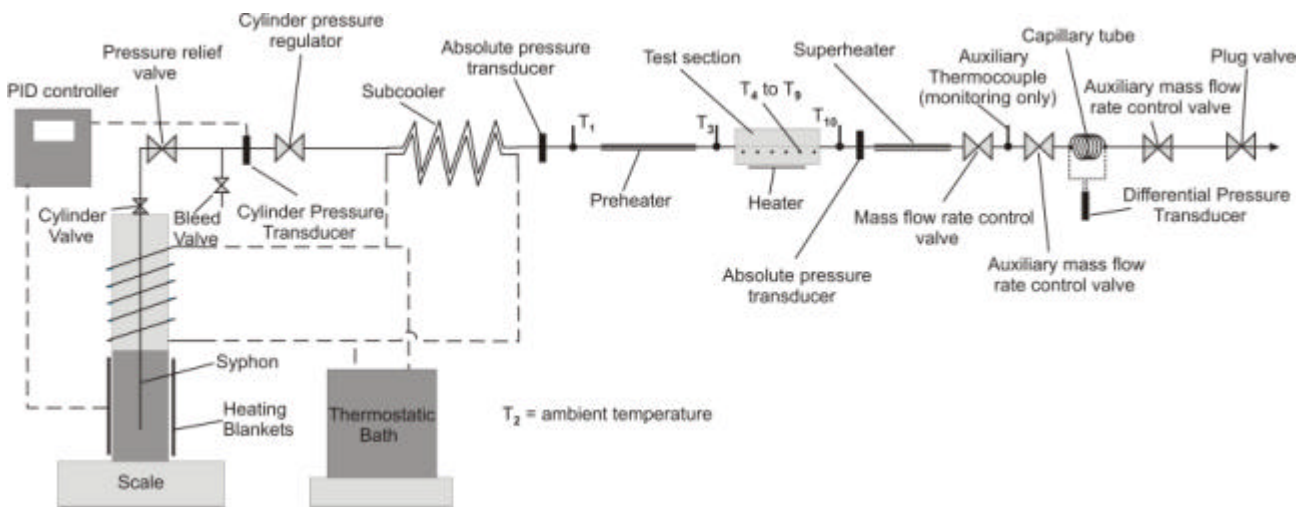


Figure 1 – Carbon dioxide open loop system

### 2.2. Control of CO<sub>2</sub> cylinder pressure

A pressure relief valve, bleed valve, and pressure transducer were placed in-line before the pressure regulator. The in-line relief valve (designed to begin opening at 10.32 MPa) ensured emergency removal of over-pressurized CO<sub>2</sub> far below the cylinder burst pressure of 41.3 MPa. The bleed valve allowed removal of the in-line pressure between the outlet and the closed cylinder valve. The pressure transducer allowed pressure measurements of the source cylinder. Two 15.5 kW/m<sup>2</sup> heating blankets were clamped to the cylinder, and used to control the pressure inside the cylinder. A copper tube heat exchanger connected to a 50% water-50% ethylene glycol temperature bath was wrapped around the CO<sub>2</sub> cylinder in order to improve the pressure control. The cylinder was then insulated with foil-faced polyethylene air pillow wrap. A control box was used to regulate and monitor the cylinder conditions with a PID (Proportional Integral Differential) feedback loop, which also provided power to the heating blankets. A variable transformer allowed variable control of the blanket heat density (0-15.5 kW/m<sup>2</sup>).

### 2.3. Control of the CO<sub>2</sub> test section inlet vapor quality

Before reaching the test section inlet the CO<sub>2</sub> flowed through a subcooler in order to permit subcooled liquid to enter the preheater. The subcooler was a copper tube counterflow heat exchanger using a 50% water-50% ethylene glycol mixture, cooled to 0°C in a temperature bath, as a heat sink. The preheater, an electric heater with a copper tube wound around it, was used to allow the saturated CO<sub>2</sub> to enter the test section inlet at a desired vapor quality. A variable transformer was used to adjust the voltage supplied to the electric heater and a digital voltmeter was used to measure the voltage. The supplied electric power was calculated by knowing the resistance of the heater. A polyethylene foam tube was utilized to isolate the preheater in order to minimize the heat transfer to the ambient. The inlet and outlet temperatures of the CO<sub>2</sub> flow in the preheater were measured by two 1.5875-mm diameter type-K thermocouples and the energy balance was

applied to determine the inlet vapor quality at the test section. A pressure transducer was used to measure the absolute pressure at the preheater inlet, which was needed to determine the inlet state of the CO<sub>2</sub> flow. Three 0.254-mm diameter type-K thermocouples were installed on the insulation surface and the temperatures measured were used to estimate the heat transfer interactions with the ambient.

#### 2.4. Control of the mass flow rate

Mass flow rates were determined by using a 1-gram resolution scale. The cylinder, including the heating blankets, insulation, and tubing, was placed on the scale and the total weight measured. As CO<sub>2</sub> exited the cylinder, the reduction in mass was measured over time. A needle valve installed after the superheater was used to throttle the flow, controlling the mass flow rate. Two other valves were installed after the needle valve to improve the mass flow rate control. Another copper-tube electric heater, named superheater, was installed with the objective of superheating the CO<sub>2</sub> before entering the needle control valve in order to avoid temperature reduction in the flow through the needle valve; otherwise it would be difficult to get a good control on the mass flow rate. In order to have an instantaneous control on the mass flow rate, it was installed a capillary tube after the control valves. The pressure drop of the CO<sub>2</sub> superheated flow through the capillary tube was used as a signal for monitoring the stability of the mass flow rate.

#### 2.5. Test section

The test section, showed in detail in Figure 2, was a rectangular microchannel milled into an aluminum substrate. Aluminum was chosen as the substrate material to model conditions within a compact heat exchanger. The section consisted of a lower frame, including the microchannel, piping, and instrumentation; a glass window that allowed for flow visualization; and an upper frame, which clamped down over the window onto the lower frame and provided a pressure seal. The 0.794-mm x 0.6858-mm x 50.8-mm microchannel had 1.6-mm diameter inlet and outlet ports bored at right angles into the substrate, allowing an o-ring groove to be milled around both ports and encircle the channel. The aluminum substrate provided three of the four microchannel walls. The fourth wall was a 6.35-mm rectangular glass window that cradled inside the lower frame. The rectangular upper frame bolted to the lower frame with 20 lockdown screws, compressing the glass onto an o-ring and providing the pressure seal. The glass window was protected from the upper frame by gasket material. The upper frame provided a 10.16-mm x 63.5-mm viewing area of the entire microchannel. Two 1.5875-mm diameter type-K thermocouples were used to measure the inlet and outlet temperatures of the CO<sub>2</sub>, and a pressure transducer was installed at the exit of the test section. A 50.8-mm x 50.8-mm square ultra-thin heating blanket (15.5 kW/m<sup>2</sup>) was attached to the back of the lower frame to provide a heat flux to the CO<sub>2</sub> in the microchannel. The entire test section was insulated using polyethylene foam to minimize heat transfer to the ambient. Three 0.254-mm diameter type-K thermocouples were installed on the insulation surface and the temperatures measured were used to estimate the heat transfer interactions with the ambient.

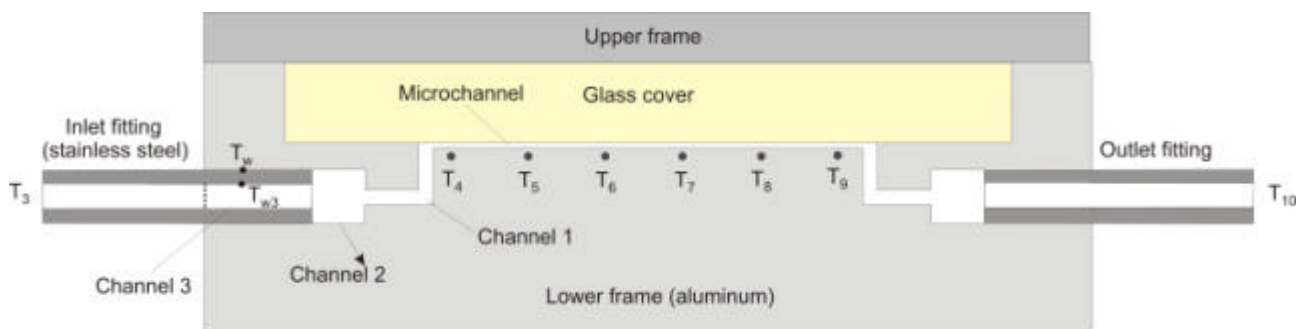


Figure 2 – Test section

#### 2.6. Running a test

The first step in running the CO<sub>2</sub> experiment was to obtain the desired pressure within the source cylinder. After adjusting the desired pressure level in the test and setting a heating value to the heating blankets, the cylinder valve was fully opened with the pressure regulator fully closed. Once the cylinder target pressure was achieved, the pressure regulator was fully opened, and CO<sub>2</sub> flowed through the subcooler and the preheater before reaching the test section inlet. CO<sub>2</sub> entered the test section at the left side through a stainless steel fitting, flowed through a 2.4-mm diameter 5 mm channel length (channel 3, still inside the fitting), and then flowed through a 6.4-mm diameter 8.8-mm channel length (channel 2), and a 1.6-mm diameter 17.0-mm channel length (channel 1) before reaching the microchannel. Then the CO<sub>2</sub> flowed within

the 50.8-mm microchannel length across the test section front towards the outlet port. The outlet-piping configuration was similar to the inlet configuration. After flowing through the microchannel, the CO<sub>2</sub> flowed through the superheater, the mass flow rate control valves, and the capillary tube, towards the line exit, and was exhausted to the ambient. All data were recorded for five minutes after the steady state regime was reached. A PC-based Data Acquisition System (DAS) was used to process transducers data collected from the test loop. During the time of data recording several photographs of the flow were taken using a digital camera.

## 2.7. Instrumentation and uncertainty

A PC-based Data Acquisition System (DAS) was used to process thermocouples and pressure transducers data collected from the test loop. A digital multimeter was used to measure voltages ( $\pm 1\%$ ) and electric resistances ( $\pm 2\%$ ). The type-K thermocouples were calibrated using a 0.1°C-resolution mercury-in-glass thermometer and a 0°C-ice bath in the temperature range from 0°C to 30°C (a reference thermocouple was placed in a Dewar flask containing finely ground ice chips and water, creating a two-phase ice bath). The uncertainty of the temperature measurements was estimated in  $\pm 0.2^\circ\text{C}$ . The manufacture-stated absolute pressure transducer and differential pressure transducer accuracies were  $\pm 0.13\%$  full scale ( $\pm 10$  kPa), and  $\pm 0.15\%$  full scale ( $\pm 0.26$  kPa), respectively.

The uncertainties of reduced data were determined by propagating the measurement uncertainties using the methodology proposed by Moffat (1988). The uncertainty of the heat supplied to the microchannel was estimated in  $\pm 0.04$  W, and the uncertainties of the mass flux,  $G$ , and vapor quality,  $x$ , were estimated in  $\pm 5\%$  and  $\pm 10\%$ , respectively.

## 3. Results and Discussion

A total of 28 experimental tests were conducted during the CO<sub>2</sub> vaporization. All tests were performed for one heating value of 1.28 W at the bottom of the test section, considering mass flux in the range of 58 to 235 kg/(m<sup>2</sup>s) and vapor qualities from 1 to 81%. The heat flux at the bottom of the microchannel was estimated at  $1800 \pm 5\%$  W/m<sup>2</sup> (2- $\sigma$  dispersion of all 28 data), and the saturation temperature was estimated at  $23.3 \pm 0.3^\circ\text{C}$  (2- $\sigma$  dispersion of all 28 data) for all tests.

Flow visualization results for all tests are given in Figures 3 to 8. Multiple photographs were taken at different times for each test while measurements were being conducted. In all these figures CO<sub>2</sub> flows from the right to the left. Using the flow regimes described by Carey (1992), three types of flow patterns were observed, namely plug, slug, and annular flow. Annular flow was assumed to be the regime when no bubbles were observed in the flow. All patterns were observed for the smaller values of mass flux (up to 149 kg/(m<sup>2</sup>s)); plug flow was predominant for low qualities (up to about 25%); slug flow was predominant for intermediate qualities (from about 25 to 50%), and annular flow was more probable for high qualities (above 50%). For mass flux of 188 and 235 kg/(m<sup>2</sup>s), only two flow patterns could be observed: slug and annular flow. Slug flow was predominant for low qualities (up to about 25%) and annular flow was more likely for high qualities. The same tendencies and flow regimes were observed by Pettersen (2001).

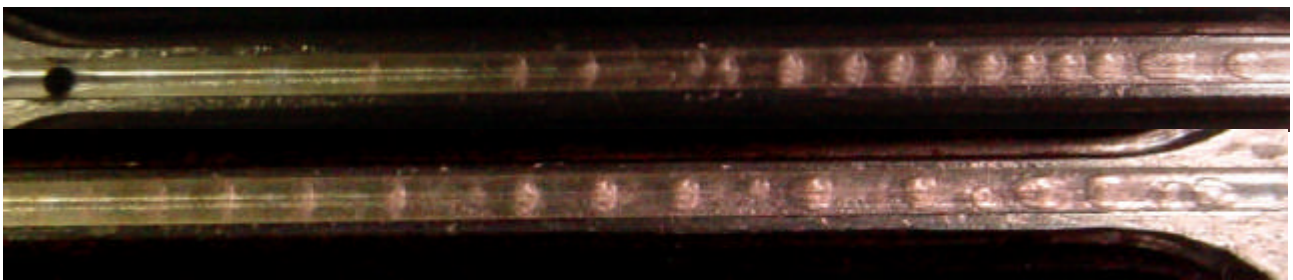


Figure 3(a) – Plug flow for  $x=13\%$

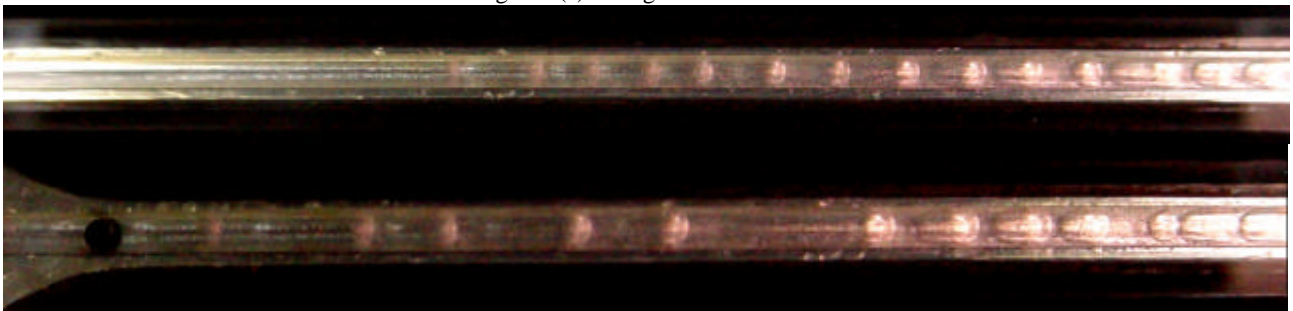


Figure 3(b) – Plug flow for  $x=16\%$

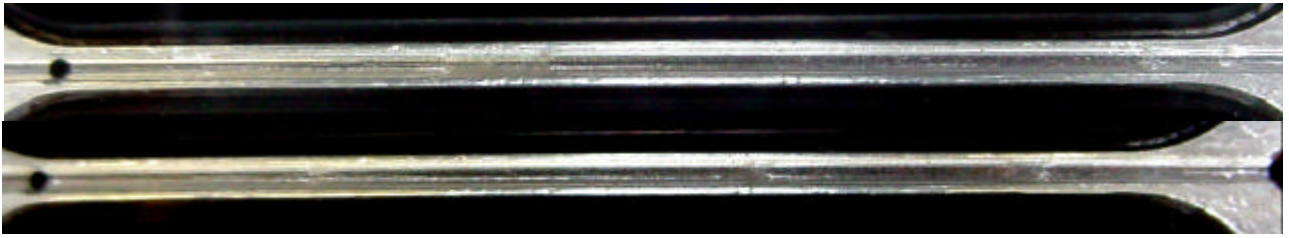


Figure 3(c) – Slug flow for  $x=48\%$

Figure 3– Flow patterns for  $G=58 \text{ kg}/(\text{m}^2\text{s})$ .

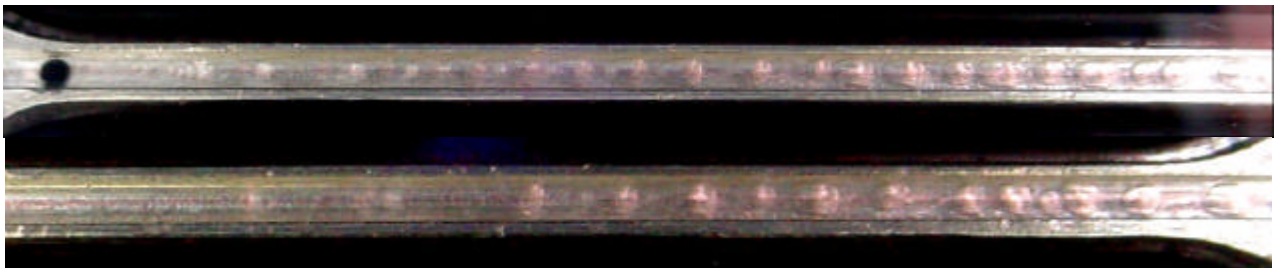


Figure 4(a) – Plug flow for  $x=6\%$



Figure 4(b) – Plug flow for  $x=25\%$

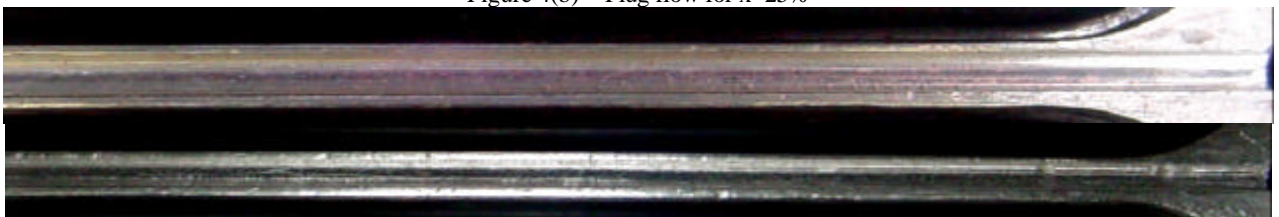


Figure 4(c) – Annular flow for  $x=52\%$

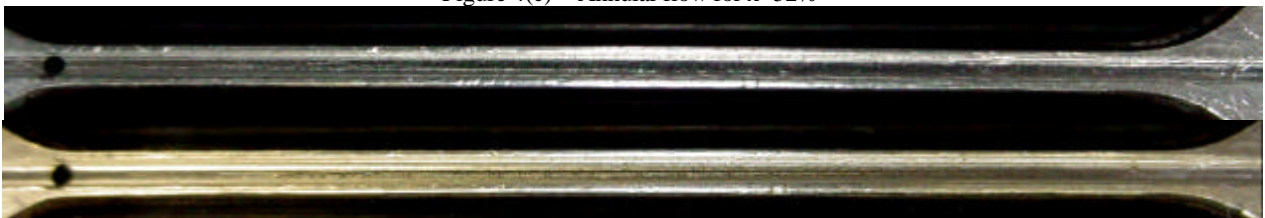


Figure 4(d) – Annular flow for  $x=66\%$

Figure 4 – Flow patterns for  $G=96 \text{ kg}/(\text{m}^2\text{s})$ .

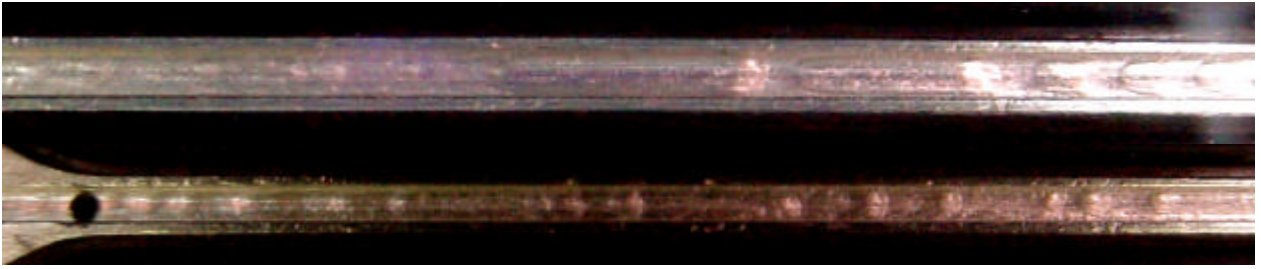


Figure 5(a) – Plug flow for  $x=2\%$

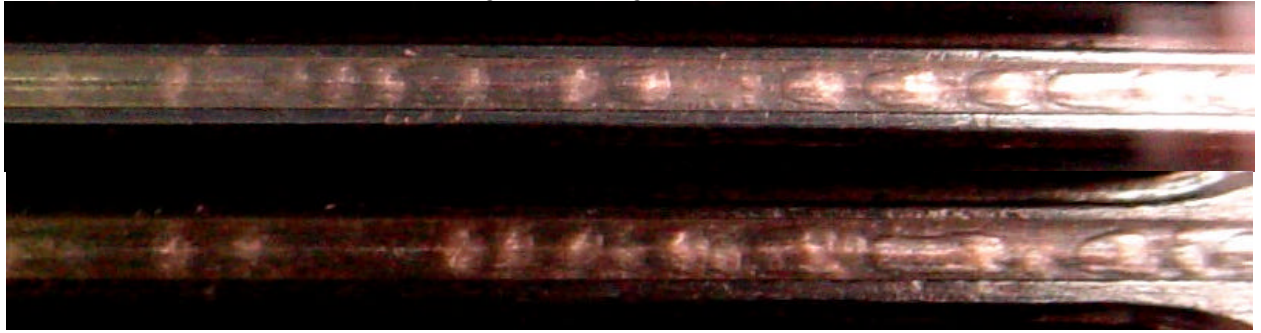


Figure 5(b) - Plug flow for  $x=15\%$

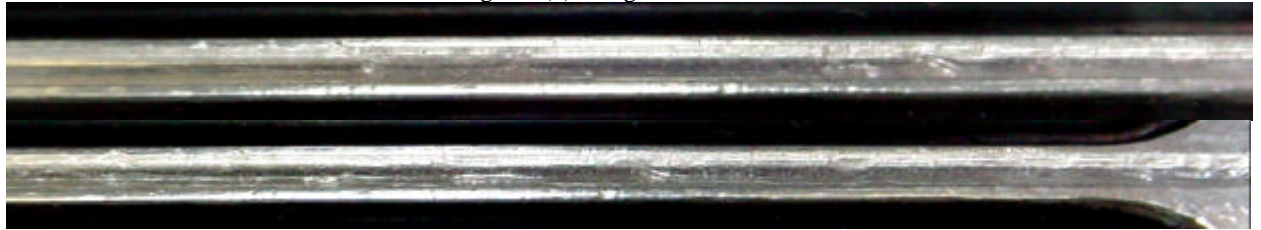


Figure 5(c) – Slug flow for  $x=36\%$

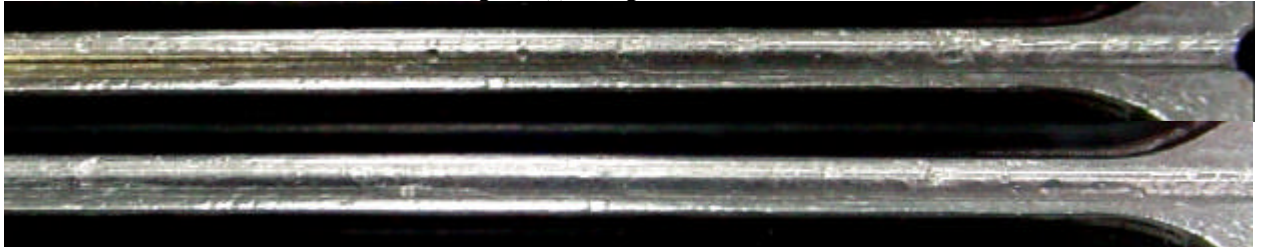


Figure 5(d) – Annular flow for  $x=61\%$

Figure 5 – Flow patterns for  $G=123 \text{ kg}/(\text{m}^2\text{s})$ .

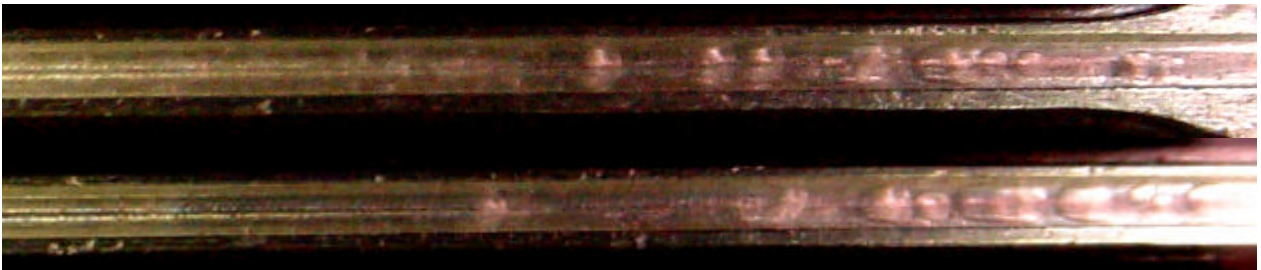


Figure 6(a) Plug flow for  $x=1\%$

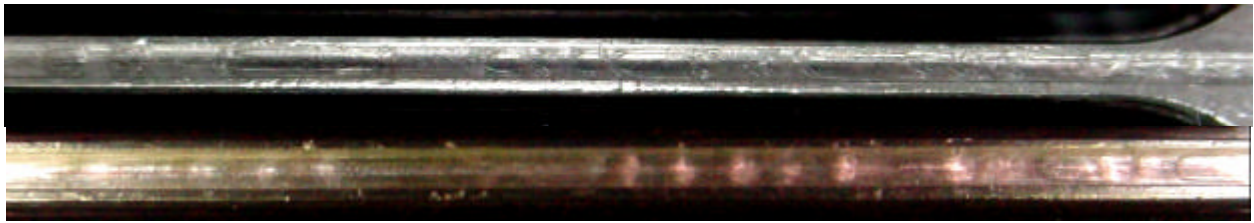


Figure 6(b) – Plug flow for  $x=13\%$

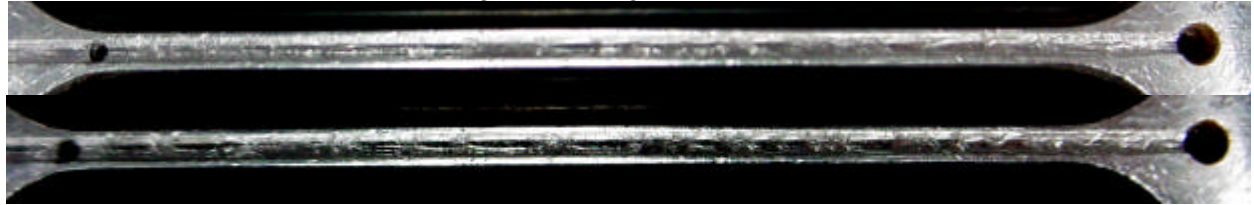


Figure 6(c) – Plug flow for  $x=25\%$

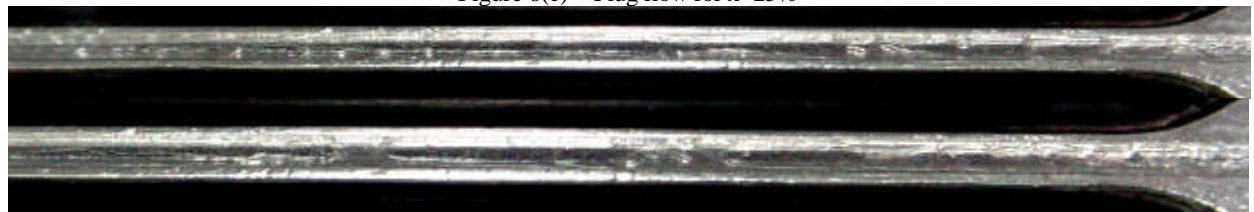


Figure 6(d) – Slug flow for  $x=29\%$

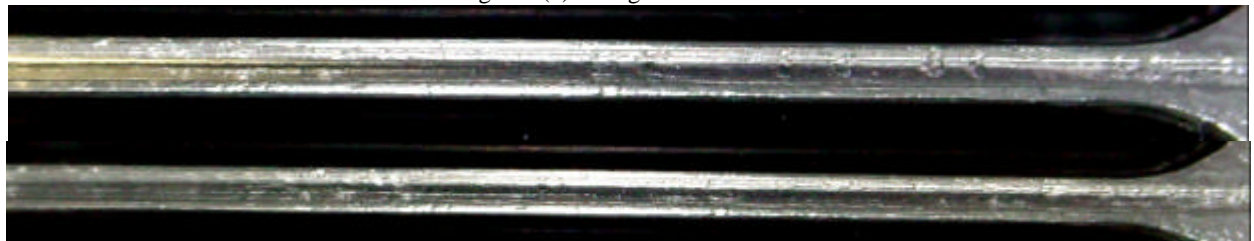


Figure 6(e) – Slug/annular flow for  $x=50\%$

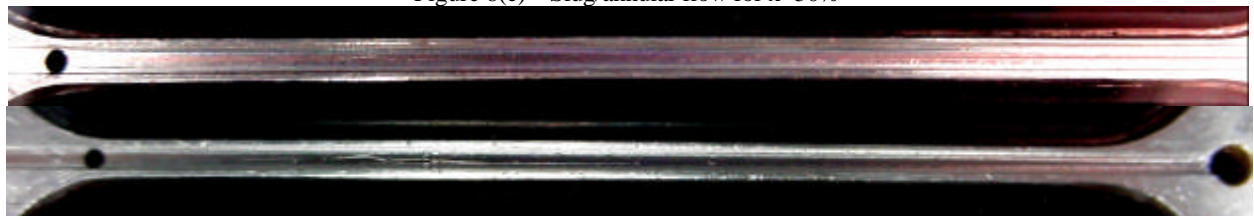


Figure 6(f) – Annular flow for  $x=73\%$

Figure 6 – Flow patterns for  $G=149 \text{ kg}/(\text{m}^2\text{s})$ .

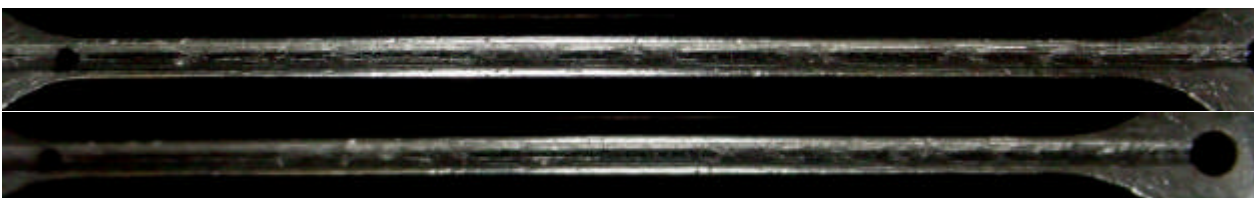


Figure 7(a) – Slug flow for  $x=12\%$



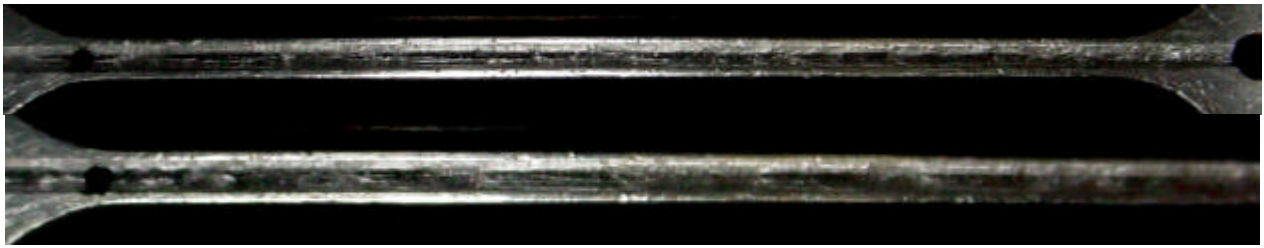


Figure 7(b) – Slug flow for  $x=25\%$

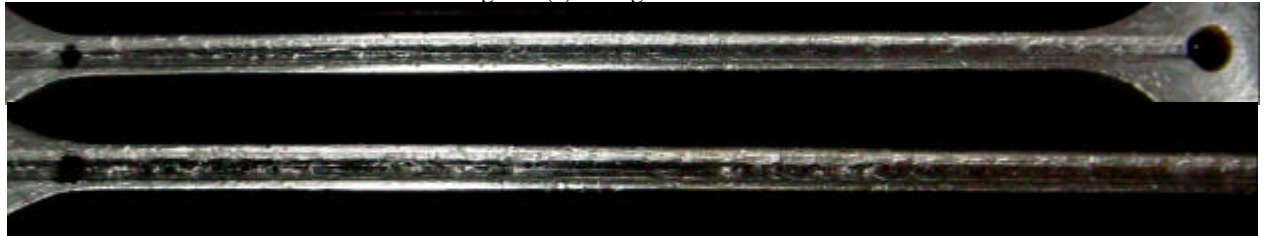


Figure 7(c) – Slug/annular flow for  $x=45\%$

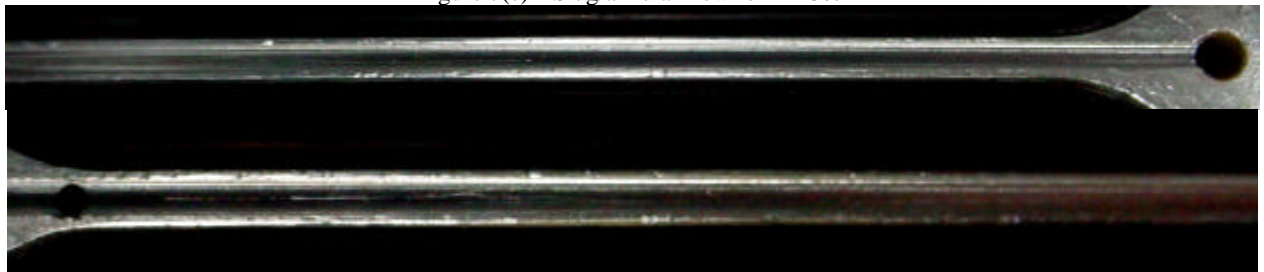


Figure 7(d) – Annular flow for  $x=67\%$

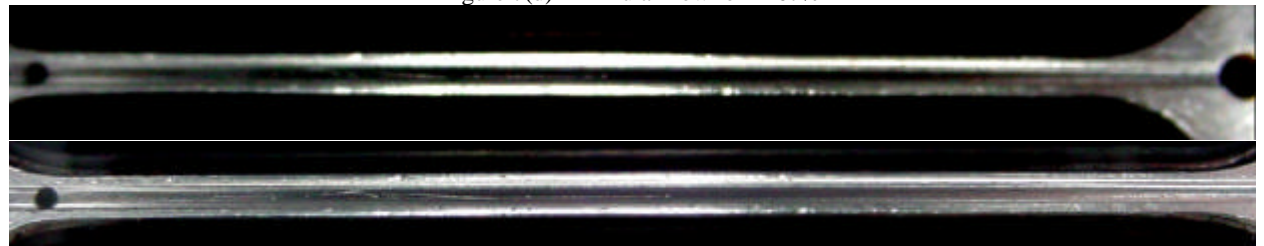


Figure 7(e) – Annular flow for  $x=79\%$

Figure 7 – Flow patterns for  $G=188 \text{ kg}/(\text{m}^2 \text{ s})$ .



Figure 8(a) – Slug flow for  $x=12\%$

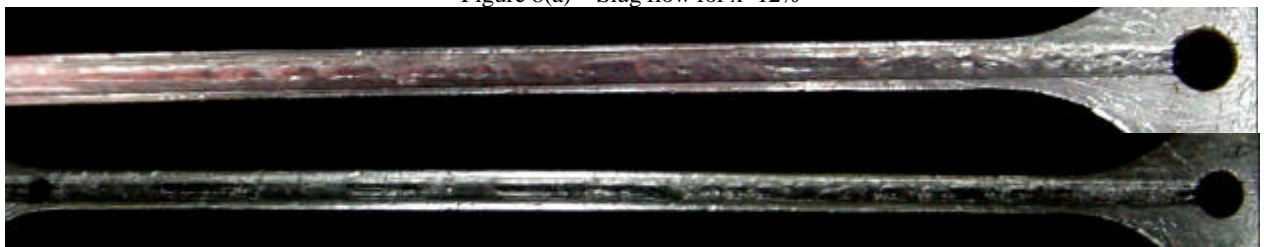


Figure 8(b) – Slug flow for  $x=25\%$

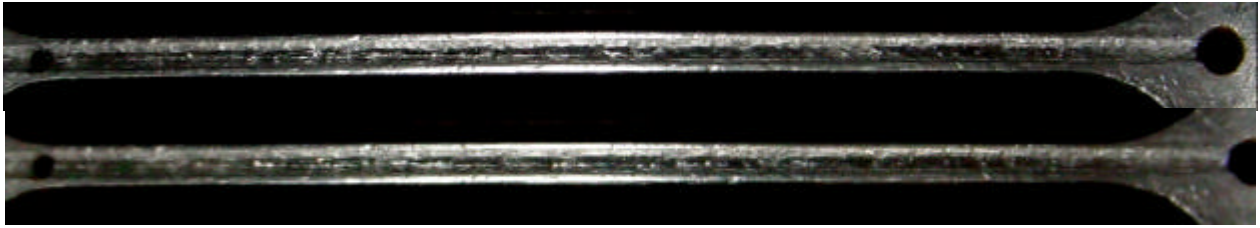


Figure 8(c) – Slug flow for  $x=41\%$

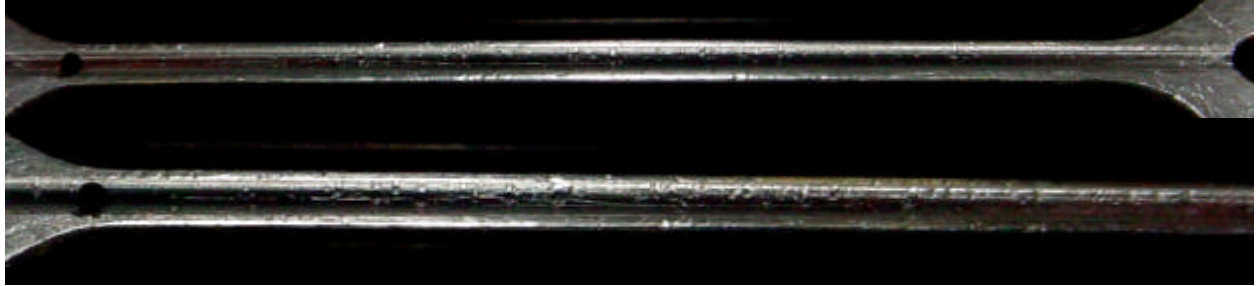


Figure 8(d) – Annular flow for  $x=59\%$

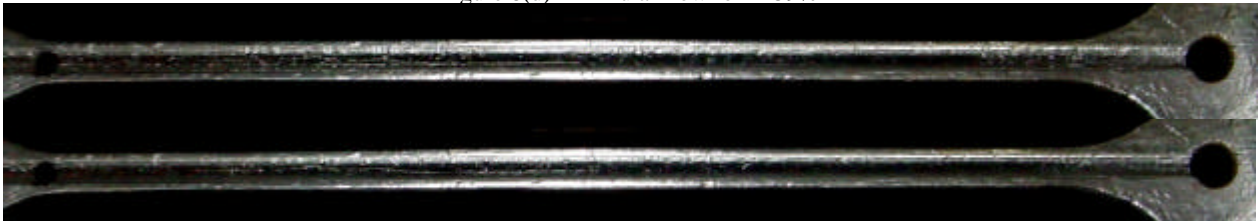


Figure 8(e) – Annular flow for  $x=71\%$

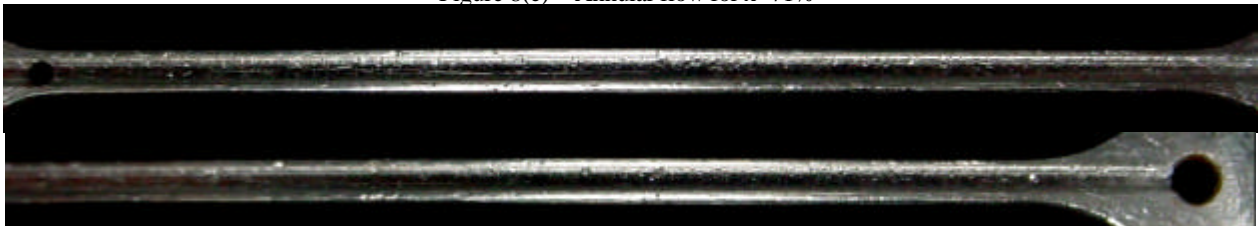


Figure 8(f) – Annular flow for  $x=81\%$

Figure 8 – Flow patterns for  $G=235 \text{ kg}/(\text{m}^2\text{s})$ .

#### 4. Summary and Conclusion

This work presents an experimental study of  $\text{CO}_2$  vaporization inside a 0.8 mm-hydraulic diameter microchannel. The visualization of the flow regimes was conducted in a total of 28 tests at saturation temperatures around  $23.3^\circ\text{C}$  for one heat flux of  $1800 \text{ W}/(\text{m}^2\text{C})$ . Vapor qualities ranged from 1 to 81% and mass flux ranged from 58 to  $235 \text{ kg}/(\text{m}^2\text{s})$ . The results showed three flow regimes. For low vapor qualities (up to about 25%), plug flow was predominant, while slug flow appeared to occur at moderated vapor qualities (from about 25 to 50%). Annular flow was theorized to be the flow pattern for higher vapor qualities.

#### 5. Acknowledgement

The author acknowledges the financial support provided by the agency FAPESP through grant 00/12567-5 and by the ACRC-Air Conditioning and Refrigeration Center, Laboratory of the Mechanical and Industrial Engineering of the University of Illinois at Urbana-Champaign, IL-USA.

#### 6. References

Aldana, J.P., Critical Heat Flux of  $\text{CO}_2$  in a Microchannel at Elevated Subcritical Pressures, (2000), MS Thesis, University of Illinois at Urbana-Champaign.

- Borishanski, V.M., (1969), Correlation of the Effect of Pressure on the Critical Heat Flux and Heat Transfer Rates Using the Theory Of Thermodynamic Similarity, in Problems of Heat Transfer and Hydraulics of Two-Phase Media, Ed. S.S. Kutateladze, pp. 16-37, Pergamon.
- Bredesen, A.M., Hafner, A., Pettersen, J., Neksa, P., Aflekt, K., 1997, Heat Transfer and Pressure Drop for In-tube Evaporation of CO<sub>2</sub>, International Conference on Heat Transfer Issues in Natural Refrigerants, College Park, MD.
- Carey, V.P., (1992), Liquid-Vapor Phase-change Phenomena: An Introduction to the Thermophysics of Vaporization and Condensation Processes in Heat Transfer Equipment, Hemisphere Publishing Co.
- Cavallini, A., (1996), Working Fluids for Mechanical Refrigeration – Invited paper presented at the 19<sup>th</sup> International Congress of Refrigeration, The Hague, August 1995, International Journal of Refrigeration, Vol. 19, n<sup>o</sup> 8, pp. 485-496.
- Gorenflo, D. (1993), Pool Boiling, In: VDI Heat Atlas (chapter Ha).
- Hihara, E., and Tanaka, S., (2000), Boiling Heat Transfer of Carbon Dioxide in Horizontal Tubes. Preliminary Proceedings of the IIR Gustav Lorentzen Conference on Natural Working Fluids, Purdue University, W. Lafayette, IN, USA, July, pp. 279-284.
- Hogaard Knudsen, H. J., Jensen, P.H., (1997), Heat Transfer Coefficient for Boiling Carbon Dioxide, IEA/IIR Workshop on CO<sub>2</sub> Technologies in Refrigeration, Heat Pump and Air Conditioning Systems, Trondheim, Norway.
- Koyama, S., Kuwahara, K., Shinmura, E., and Ikeda, S., (2001), Experimental Study on Flow Boiling of Carbon Dioxide in a Horizontal Small Diameter Tube, IIR Conference on Thermophysical Properties and Transfer Processes of New Refrigerants, October 3-5, Paderborn, Germany.
- Moffat, R.J., (1988), Describing the Uncertainties in Experimental results, Experimental Thermal and Fluid Science, Vol. 1, pp. 2-17.
- Ohadi, M., Molki, M., and Zhao, Y., (2000), CO<sub>2</sub> Heat Transfer and Fluid Flow, Workshop on Vapor Compression with the Critical Point in Mind, University of Maryland.
- Palm, B., (2001), Heat Transfer in Microchannels, Microscale Thermophysical Engineering, Vol. 5, pp. 155-175.
- Pettersen, J., Hafner, A., Skaugen, G., and Rekstad, H., (1998), Development of Compact Heat Exchangers for CO<sub>2</sub> Air-conditioning Systems, International Journal of Refrigeration, Vol. 21, n<sup>o</sup> 3, pp. 180-193.
- Pettersen, J. (2001), Flow Vaporization of CO<sub>2</sub> in Microchannels Tubes. Doctor Technicae Thesis. Norwegian University of Science and Technology. Faculty of Mechanical Engineering. Department of Refrigeration and Air Conditioning. 249 pp.
- Rieberer, R., (1998), CO<sub>2</sub> as Working Fluid for Heat Pumps. Revised copy of doctoral thesis submitted to the Faculty of Mechanical Engineering, Graz University of Technology, December.
- Sun, Z., and Groll, E., (2001), CO<sub>2</sub> Flow Boiling in Horizontal Tubes, Ray W. Herrick Laboratories, Purdue University, Internal Report #229.HL-2001-8, W. Lafayette, Indiana, USA, April.
- Thome, J., (2001), On Recent Advances in Modelling of Two-phase Flow and Heat Transfer, Proc. 1<sup>st</sup> International Conference on Heat Transfer, Fluid Mechanics and Thermodynamics, 8-10 April, Kruger Park, South Africa, pp. 27-39.
- Yun, R., Hwang, J.H., Kim, Y.C., and Kim, M.S., (2001), Evaporation Heat Transfer Characteristics of Carbon Dioxide in a Horizontal Smooth Tube, IIR Conference on Thermophysical Properties and Transfer Processes of New Refrigerants, October 3-5, Paderborn, Germany.
- Zhao, Y., Molki, M., Ohadi, M.M., Dessiatoun, S.V. (2000), Flow Boiling of CO<sub>2</sub> in Microchannels, ASHRAE Transactions: Symposia, Vol. 106, Part 1, pp. 437-445.